Neoproterozoic metamorphic events in the kekem area (central domain of the Cameroon north equatorial fold belt): P-T data.

TCHAPTCHET TCHATO D.[c], NZENTI P. [a], NJIOSSEU E. L.[a], NGNOTUE, T.[b], GANNO S.[a]

[a] Laboratory of Structural Geology and Petrology of Orogenic Domains (LPGS), Department of Earth Sciences, Faculty of Sciences, P.O.Box 812, University of Yaoundé I, Cameroon.

[b] Department of Earth Sciences, Faculty of Sciences, University of Dschang, Cameroon.

[c] Laboratoire d'analyse des matériaux (MIPROMALO), B.P. 2396 Yaoundé.

ABSTRACT

The Kekem area (southwestern part of the central domain of the Cameroon North Equatorial Fold Belt) is composed of high-grade migmatitic gneisses in which two lithological units are distinguished: (i) a metasedimentary unit (garnet- sillimanite-biotite-gneisses and garnet-biotite-gneisses) interpreted as a continental series; and (ii) meta-igneous rocks comprising mafic pyroxene gneisses, amphibolites, and orthogneisses. These units recrystallised under HT-MP conditions (T=700-800°C, P $\geq$ 0.5-0.8GPa) and were deformed in relation to a major tangential tectonic event with the NNE-SSW kinematic direction. The lithological association and its tectono-metamorphic evolution show striking similarities with the Banyo and Maham III gneisses, suggesting that the extensional depositional environment envisaged for this formation can be extended farther west. P-T calculations in this contribution provide new data on the Pan-African structural and metamorphic evolution of the metapelites and metabasites in the basement of the Kekem area. The results show two distinct events: (1) crystallization during a Pan-African high temperature metamorphic event and, (2) subsequent deformation and high temperature mylonitization. The data imply a high-temperature amphibolite-facies metamorphism along a clockwise P-T path. The recorded P-T involves a marked variation in pressure, which is typical of collisional crustal thickening. The contrasted metamorphic evolution between areas located to the south of the Central Cameroon Shear Zone (CCSZ; high pressure: Yaoundé, Ntui-Betamba), and those located to the north (low pressure: Banyo, Tibati), along with widespread remains of Paleoproterozoic crust, suggest important crustal thickening during Pan-African tangential tectonics in southern Cameroon. As a consequence, the CCSZ is not simply a late Pan-African transpressive shear zone but appears to have been formerly a major intracontinental thrust zone.

Key words: HT metamorphic event / Kekem/ Cameroon / Collisional crustal thickening / Neoproterozoic / North Equatorial Fold Belt.

RESUME

La région de Kekem est formée de gneiss anatectiques de haut-degré dans lesquels deux ensembles sont reconnus: (i) un ensemble métasédimentaire (gneiss à grenat, sillimanite et biotite, et gneiss à grenat et biotite) considéré comme déposé à l´intérieur d´un continent, (ii) des roches méta-ignées comprenant des gneiss à grenat et pyroxène, des amphibolites de composition mafique, et des orthogneiss. Ces deux ensembles ont recristallisé (T=700-800°C, P $\geq$ 0,5-0,8GPa) et ont été déformés en relation avec un épisode majeur de tectonique tangentielle de direction cinématique NNE-SSW. Cette association lithologique et son évolution tectono-métamorphique montrent une similitude remarquable avec les formations panafricaines de Banyo et Maham III du domaine central de la chaîne, suggèrant que le contexte extensif de dépôt envisagé pour ces dernières peut être étendu plus à l´ouest. Les données nouvelles sur l´évolution tectono-métamorphique des métasédiments et des métabasites panafricains du socle de la région de Kekem mettent en evidence un métamorphisme panafricain de haute température suivi d´une mylonitisation à haute température dans le faciès amphibolite de haut degré selon un chemin P-T horaire. Les conditions P-T enregistrées se caractérisent par une variation de pression typique d´un épaississement crustal. L´évolution métamorphique panafricaine contrastée entre le domaine au sud du cisaillement Centre Camerounais (CCC; haute pression: Yaoundé, Ntui-Bétamba) et le domaine nord-CCC (basse à moyenne pression: Banyo, Tibati) ainsi que la présence ubiquiste de reliques d´une croûte ancienne paléoprotérozoïque, suggèrent un important épaississement crustal, lors d´un épisode de tectonique tangentielle. Le CCC n´est donc pas un simple accident panafricain transpressif, mais apparaît bien avoir été préalablement un chevauchement intracontinental majeur.

Mots-clés : Métamorphisme de Haut degré / Kekem / Cameroun / Epaississement crustal / Néoprotérozoïque / Chaîne Nord Equatoriale

Epreuves à : Jean Paul NZENTI, Université de Yaounde I, Faculté des Sciences, Laboratoire de Pétrologie et Géologie Structurale, B.P. 3412 Messa-Yaounde, Cameroun. Phone: 00 (237) 99 93 91 57
e-mail: jnzenti@yahoo.com

1. INTRODUCTION

The Kekem area (Figs 1 & 2) is located in the southwestern part of the Cameroon central domain in the North equatorial fold belt (Nzenti et al., 1988) or Central African fold belt (Toteu et al., 2001). Although the southern limit of the Yaoundé series towards the Congo craton is rather well defined, its northern extension towards the Adamawa area is still poorly known. The North-Equatorial Fold Belt or Central African Orogen is a major Neoproterozoic Orogen linked to the Trans-Saharan belt of western Africa and to the Braziliano Orogen of northeastern Brazil (Fig 1a). In Cameroon, the Neoproterozoic realm (Nzenti et al., 1994; 1998; 2006; Ngnotué et al., 2000; Tanko Njiosseu et al., 2005) is made up of three domains from south to north (Fig 1b):

(i) The southern domain comprises Neoproterozoic metasedimentary units, such as the Ntui-Betamba , Yaoundé and Mbalmayo units; the protoliths of these units were deposited in a passive margin environment at the northern edge of the Congo craton and were metamorphosed under high P conditions at 616 Ma (Ngnotué et al., 2000; Nzenti et al., 1988; Penaye et al., 1993). An alkaline magmatism (Nzenti, 1998) was also recognized in association with these Neoproterozoic units. The rocks of this southern domain were thrust onto the Archean Congo craton towards the south (Nzenti et al., 1984; 1988; Nedelec et al., 1986). The thrust continues towards the east, forming the Oubanguides Nappe in the Republic of Central Africa;

(ii) The central domain lies between the Sanaga fault to the south and the Tcholliré-Banyo fault to the north.

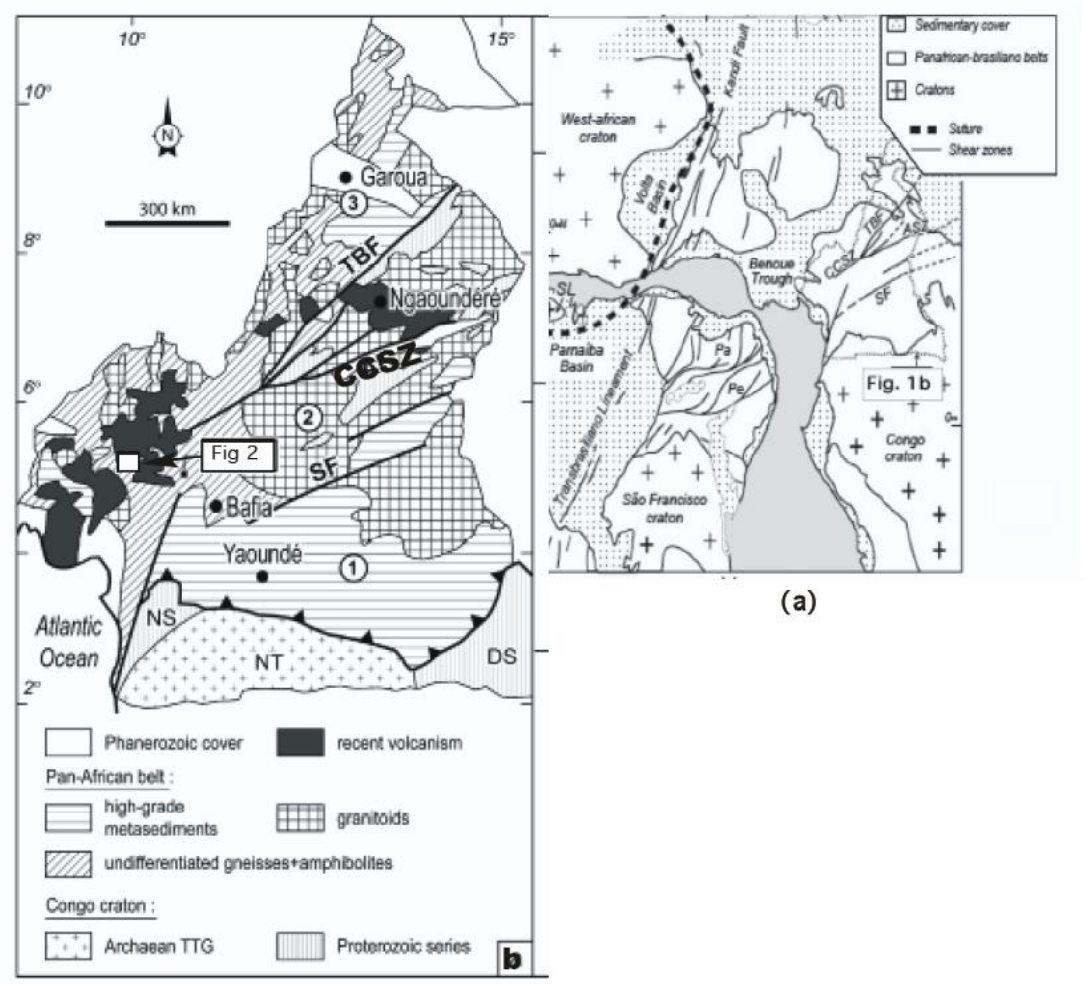

Fig 1: (a) Geologic reconstruction of Africa and NE Brazil (late Precambrian) after Caby et al., (1991). CCSZ: Cameroon Central Shear Zone; SF: Sanaga fault; SL: São Luis Craton; Pa: Patos shear zone; Pe: Pernambuco shear zone; TBF: Tibati-Banyo Fault and **(b)** geological map of Cameroon with the three main domains of the Pan-African orogenic belt (modified from Soba, 1989; Nzenti et al., 1994) and adapted from Ngnotué et al., 2000, Tanko Njiosseu et al., 2005 and Nzenti et al., 2006: (1) southern domain corresponding to the Yaoundé series thrust on the Congo Craton, (2) central domain, (3) northern domain; Granitoids groups are not distinguished due to large scale. TBF: Tibati-Banyo Fault, SCSZ: Southwestern Cameroon shear zone, CCSZ: Central Cameroon Shear Zone, SF: Sanaga Fault. NT: Ntem complex; DS: Dja series; NS: Nyong series. Location of study area is marked by a square. Inset shows location of Fig 2.

These large NE-striking transcurrent faults, as well as the Adamaoua fault inside the central domain, are regarded as possible prolongations of the major shear zones of NE Brazil in a pre-drift Gondwana reconstruction (Castaing et al., 1994). This central domain consists of high-grade gneisses intruded by widespread Neoproterozoic syntectonic plutonic rocks of high K calc alkaline affinities (Nguiessi et al., 1997; Nzenti et al., 1994; 2006; Tagne Kamga et al., 1999; Nzolang et al., 2003; Tanko Njiosseu et al., 2005);

(iii) The northern domain consists of subordinate 830 Ma-old volcanics of tholeiitic and alkaline affinities associated with metasediments known as the Poli series. Widespread 630-660 Ma-old calc-alkaline granitoids, presently orthogneissified, result from a major episode of crustal accretion. A Paleoproterozoic crustal source in this region is attested by the presence of ~2Ga old inherited zircons in the granitoids (Toteu et al., 1987).

Clarifying the northward extension of the high pressure Yaoundé series, distinction of the different portions of the crust with different ages, therefore, are needed for understanding the orogenic assembly of the North Equatorial Fold Belt in Cameroon and allow for a better understanding of the geodynamic significance of the fold belt to the north of the Archean Congo-Sao Francisco Craton. The aim of the present study is to provide new data on the Pan-African structural and metamorphic evolution in the metapelites and metabasites in the basement using detailed mineral chemistry in combination with quantitative geothermobarometry. This study is concentrated on metamorphosed sedimentary and basic rocks of the Kekem area considered as Pan-African rocks (582 to 552 ± 15 Ma, Th-U-Pb on monazite EMP dating; Tchaptchet et al., 2008 in press). The present paper shows that all metasediments and metabasites of the Kekem area have experienced high temperature metamorphic

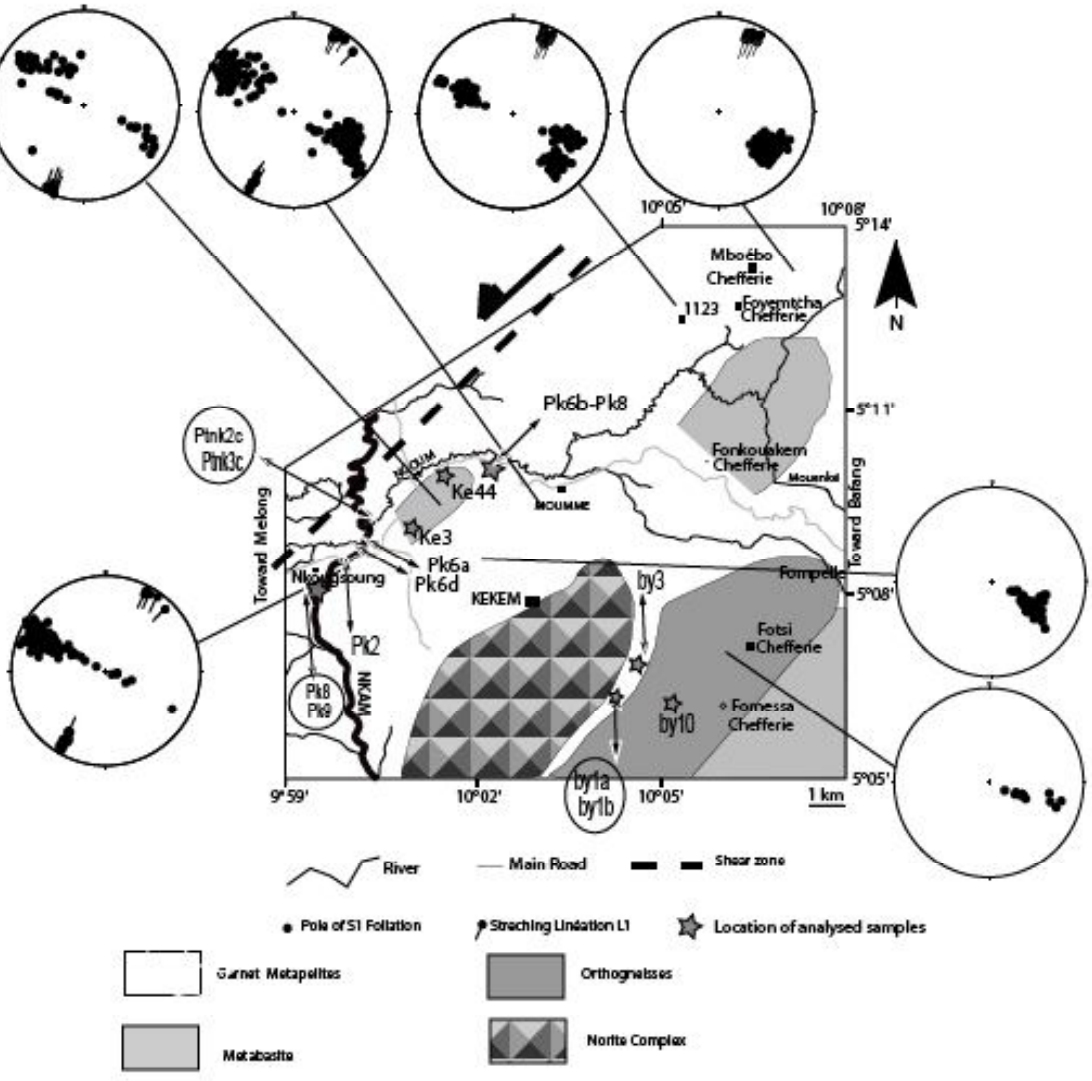

Fig 2: Geological and tectonic map of the Kekem region.

event and, subsequent deformation and high temperature mylonitization during Neoproterozoic times. The data imply a high-temperature amphibolite-facies metamorphism along a clockwise P-T path, which is typical of collisional crustal thickening.

2. GENERAL GEOLOGY

The Kekem area (231 km^2, Fig 2; Tchaptchet, 2000 and 2001) belongs to the southwestern part of the central domain. The area is formed of two distinct lithotectonic sets: a metamorphic set and a magmatic set. The metamorphic set is composed of metabasites (mainly garnet-pyroxene gneisses, amphibolites and pyroxenites) and metasediments (mainly garnet-biotite/sillimanite gneisses, garnet-biotite gneisses). Garnet-pyroxene gneisses are the dominant rock type in the magmatic set and occur, more particularly, as a large body (Fig 3c) in the NW of the study area (Fig 2), around Nkam bridges and sometimes as flagstones or boudins (30cmx50cmm) inside the garnet -biotite gneisses (Fig 3a). Their contacts with the metasediments are unexposed, and it is difficult to ascertain whether they are intrusive in the metasediments. All these rocks outcrop as inselberg, flagstones, lenses or boudins. Granoblastic textures prevail in all rock types, although flaser and mylonitic ones are also commonly observed. It records a first phase of deformation D1, underlined by a sub horizontal foliation parallel to the compositional layering (Fig 3a). The magmatic set comprises more or less orthogneissified granitoids, which crop out close to shear zones characterizing the second phase of deformation D2 and were emplaced during D2, and post D2 granitoids (biotite- and amphibole- rich granites, two micas granites, monzodiorite, monzonite and norite). The S2 foliation planes are mildly to steeply dipping and strike N40°E in average; they are axial planes of the F2 fold and underlined by stretched crystals of quartz, biotite flakes

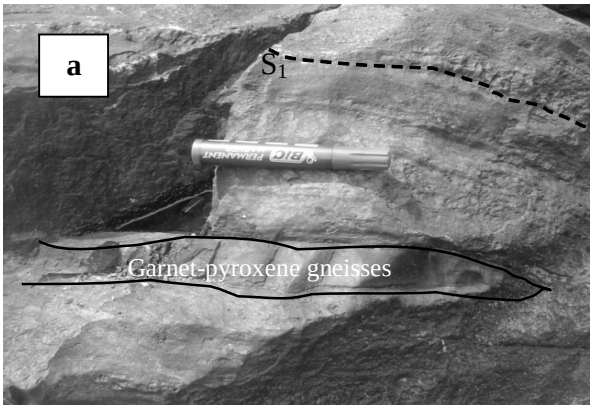

Strongly foliated garnet-sillimanite gneisses

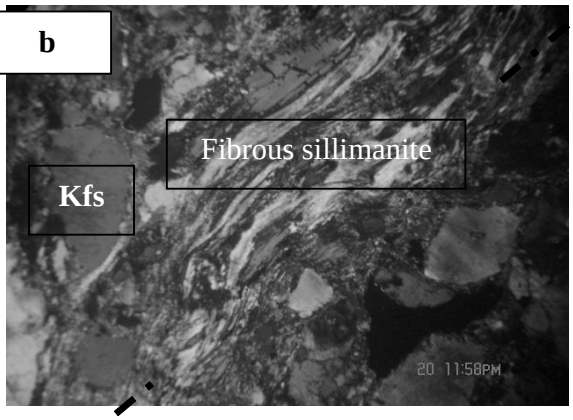

S_1

Large body of the garnet-pyroxene gneisses

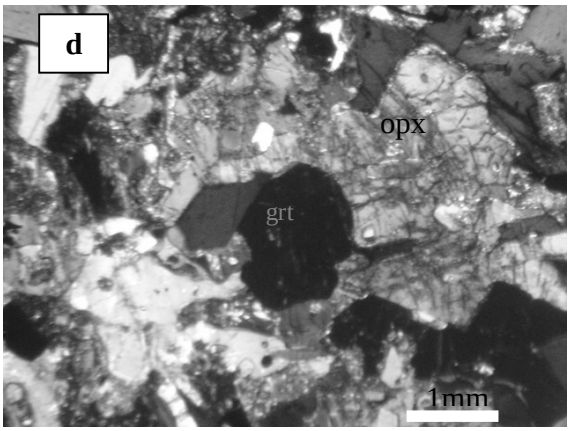

Photomicrograph (crossed polars) from a garnet – pyroxene gneisses (sample pk2). Mineral abbreviations after Kretz (1983).

Fig 3: Microsructures in garnet-biotite/sillimanite-gneisses and garnet-pyroxene gneisses of the Kekem area.

and by injected granitic veins. To study and characterize these metamorphic rocks is of major importance in constraining the geodynamic models speculating on the existence of an older crust reworked during Neoproterozoic orogenesis (Toteu *et* al., 2004).

3. METHODS OF INVESTIGATION

The Kekem area was mapped and samples collected for laboratory studies. In this study >100 thin sections of metasediments and metabasites were petrographically investigated. Selected mineral assemblages of these rocks are given in Table 1. Electron microprobe studies were carried out on: (i) the automated CAMEBAX electron microprobe at the Göttingen Zentrum Geowissenschaften, University of Göttingen in Germany. The equipment was operated at 15Kv, 10nA, and using the MBXCOR correction procedure (Henoc and Tong, 1978) and (ii) an electron microprobe JEOL JXA8900 RL hosted at the Institut für Werkstoffwissenschaft at Freiberg/ Saxony in Germany. The analytical conditions were 20 kV, 20 A and the common matrix ZAF corrections were applied. Garnets and plagioclases were analyzed along transgranular profiles composed of several points. Biotite was characterized by analyses from cores and rims. As recasted, ferric iron always remains very low and does not significantly affect precision of P-T estimates (currently ± 50°C and ± 1Kbar). Microprobe analyses (30 of garnet, 8 of pyroxene, 27 of feldspar and 26 of biotite) of selected minerals are given in Tables 2 -5. Mineral abbreviations are according to Kretz (1983). Fifteen representative samples were selected for chemical analysis (Table 6). Major elements were analyzed by inductively coupled plasma atomic emission spectrometry (ICP-AES), and trace elements by inductively coupled plasma mass spectrometry (ICP-MS) on a VG-Plasma Quad STE ICP mass spectrometer at Göttingen Zentrum Geowissenschaften, University of Göttingen in Germany. The samples were dissolved in a Teflon pressure bomb, using a 1:1 mixture of HF and HClO4 at 180°C, and then taken up in HNO3 solution with an internal standard. After dissolution in HF-HClO4, the samples were taken up in a mixture of HNO3, 6N HCl and HF and diluted. These solutions were measured within 24 hours after dilution, to prevent absorption of high field strength elements (HFSE) on the sample bottle. All Hf and Ta concentrations reported in this study (Table 6) were determined following this procedure. Analytical uncertainties are currently better than 1% for major elements and 5-10% for trace element concentrations. Analytical precision for rare earth elements (REE) is estimated at 5% for concentrations >10ppm and 10% when lower. Most samples were

Table 1: Selected mineral assemblages and their modal compositions (vol %) of the main metasedimentary and metabasites rocks from the Kekem area.

Metasedimentary rocks	
garnet-sillimanite gneisses	quartz (20-30), K-feldspar (Or_{91}-Or_{95}; 20-35), plagioclase (An_{30-42}; 10-15), garnet (X_{Fe} = 0.61-0,71; 10-15), sillimanite (5-15), biotite (X_{Mg} = 0.51-0.63; 5-10).
Garnet-biotite gneisses	quartz (15-35), plagioclase (An_{35-45}; 25-35), K-feldspar (Or_{90}-Or_{93}; 5-15), muscovite (5-20), garnet (5-15), biotite (≤5).
Meta-igneous rocks	
Garnet-pyroxene gneisses	quartz (10-15), plagioclase (An_{87-88}; 15-25), orthopyroxene (X_{Fe} = 0.59-0.60; 20-30), clinopyroxene (X_{Fe} = 0.46-0.47; 5-10), garnet (X_{Fe} = 0.65-0.66; 5-10), biotite (X_{Fe} = 0.58-0.60; 10-15), K-feldspar (Or_{95}-Or_{98}; ≤5), ferro-pargasitic hornblende (5-10).
Amphibolites	quartz (≤10), plagioclase (An_{15-20} ; 20-30), K-feldspar (≤10), biotite (X_{Mg} = 0.61-0.68), ferro-hornblende (50-60).
pyroxenites	orthopyroxene (55-65), garnet (15-20), quartz (≤3), magnetite (5-15).

Table 2 : Representative chemical compositions of garnet (STRUCTURAL FORMULAE : 24 Oxygens and 16 Cations).

Sample	Pk6b										Pk8													Pk2				
Analys.	4	5	6	8	9	11	13	23	38	41	98	99	100	101	102	104	105	108	115	116	117	118	119	120	50	51	52	53	54
SiO_2	37,84	37,75	37,61	38,18	39,00	38,47	38,98	38,20	38,00	37,86	37,91	37,65	37,93	38,12	38,61	38,62	38,74	38,92	38,06	38,19	37,84	37,83	38,15	37,90	37,4	37,5	37,1	37,4	37,4
Al_2O_3	21,59	21,65	22,05	25,79	25,38	25,53	26,28	26,93	21,22	21,49	21,84	21,65	21,53	21,59	21,56	21,76	21,72	21,67	21,62	21,75	21,66	21,50	21,67	21,54	21	20,9	21,1	21,2	21,2
FeO	30,10	29,74	28,93	5,06	5,14	5,06	5,26	5,45	31,17	32,19	31,31	31,18	29,78	26,56	25,75	26,27	26,15	26,78	28,01	29,06	29,52	29,96	30,50	30,88	30	30,3	30,6	30,6	30,6
MnO	0,77	0,78	0,74	8,14	8,27	8,35	7,55	6,70	0,86	0,92	0,87	0,83	0,70	0,64	0,64	0,70	0,64	0,68	0,77	0,79	0,69	0,77	0,78	0,81	0,75	0,82	0,85	0,8	0,9
MgO	5,97	6,07	6,09	0	0	0	0	0	5,66	5,29	5,24	5,93	6,19	5,38	5,30	5,42	5,24	5,57	5,95	6,09	6,92	6,36	6,35	5,73	3,19	3,17	3,03	2,96	2,94
CaO	3,16	3,64	3,97	0,01	0,00	0,00	0,00	0,00	2,61	2,37	2,57	2,48	3,10	6,92	7,61	7,23	7,19	6,33	4,90	3,63	2,91	2,72	2,55	2,33	7,21	7,25	7,2	7,08	7,07
Total	99,5	99,7	99,4	99,4	99,7	99,8	100,0	99,7	99,6	100,2	99,7	99,7	99,2	99,2	99,5	100,0	99,7	100,0	99,3	99,5	99,5	99,1	100,0	99,2	99,57	99,9	99,96	100,0	100,1
Si	2,99	2,97	2,96	2,99	3,04	3,00	3,03	2,99	3,01	2,99	2,99	2,98	2,99	3,00	3,02	3,01	3,02	3,03	2,99	3,00	2,97	2,99	2,99	3,00	5,98	5,98	5,93	5,96	5,97
Al	2,01	2,01	2,05	1,99	1,95	1,99	1,96	2,00	1,98	2,00	2,03	2,02	2,00	2,00	1,99	2,00	2,00	1,99	2,00	2,01	2,01	2,00	2,00	2,01	3,95	3,93	3,98	3,98	3,98
Fe	1,99	1,96	1,90	1,69	1,65	1,67	1,71	1,76	2,06	2,13	2,07	2,06	1,97	1,75	1,68	1,71	1,71	1,74	1,84	1,91	1,94	1,98	2,00	2,05	4,00	4,05	4,09	4,08	4,08
Mn	0,05	0,05	0,05	0,04	0,04	0,04	0,04	0,05	0,06	0,06	0,06	0,06	0,05	0,04	0,04	0,05	0,04	0,05	0,05	0,05	0,05	0,05	0,05	0,05	0,10	0,11	0,12	0,11	0,12
Mg	0,70	0,71	0,71	0,59	0,60	0,59	0,61	0,64	0,67	0,62	0,62	0,70	0,73	0,63	0,62	0,63	0,61	0,65	0,70	0,71	0,81	0,75	0,74	0,68	0,76	0,75	0,72	0,70	0,70
Ca	0,27	0,31	0,33	0,68	0,69	0,70	0,63	0,56	0,22	0,20	0,22	0,21	0,26	0,58	0,64	0,60	0,60	0,53	0,41	0,31	0,25	0,23	0,21	0,20	1,23	1,24	1,23	1,21	1,21
Alm%	66	64	63	56	55	56	57	58	68	70	70	68	65	58	56	57	58	59	61	64	63	66	66	69	65	65	65	66	66
Grs	9	10	11	23	23	23	21	19	8	7	7	7	9	19	21	20	20	18	14	10	8	8	7	7	21	21	21	20	20
Prp	24	24	24	20	20	20	20	21	22	21	21	23	24	21	21	21	21	22	23	24	27	25	25	23	13	13	12	12	12
Sps	1	2	2	1	2	1	3	2	2	2	2	2	2	2	2	2	1	1	2	2	2	1	2	1	2	2	2	2	2

Pk6b, Pk8 : Garnet-sillimanite-biotite gneisses. Pk2 : Garnet-pyroxene gneisses

also analyzed for major and trace element concentrations by X-ray fluorescence spectrometry (XRF; Phillips PW 1840 on fused glass pellets) at the University of Göttingen. Precision for these measurements is better than 1% for major elements, and better than 5% for trace elements including Rb, Sr, Sm and Nd (Hartmann, 1994). Discrepancy between the two techniques for major elements was typically of the order of 1-2%, and never exceeded 5%.

4. RESULTS AND INTERPRETATIONS

4-1 Structures and optical mineralogy

The early phase of deformation (D1) is represented by a foliation S1, commonly flat-lying and striking N30°E (Fig 2), outlined by a compositional layering and by the preferred orientations of biotite lamellae, sillimanite, feldspar and pyroxene crystals and amphibole fishes. This plane, locally mylonitic, moulds garnet porphyroblasts. The L1 mineral and stretching lineation trends N0-20°E with nearly horizontal plunge

Table 2 : Chemical composition of orthopyroxene, clinopyroxene and structurale formulae (6 oxygens) from the garnet- pyroxene gneisses (Pk2)

Sample	Pk2			Opx			Cpx	
Analyses	36	37	38	39	42	43	40	41
SiO2	49,5	49,4	49,9	49,1	49,3	49,1	51	51,3
Al2O3	0,71	0,7	0,78	0,82	0,8	0,76	1,29	0,91
TiO2	0,11	0,11	0,09	0,14	0,14	0,08	0,175	0,14
FeO	35,3	35,3	35,2	34,9	34,9	35,4	15,52	14,3
MnO	0,65	0,69	0,79	0,76	0,72	0,75	0,261	0,27
MgO	12,6	12,5	12,4	12,7	12,7	12,5	9,85	10,4
CaO	0,84	0,93	0,95	1,09	1,04	1,03	21,72	22,6
Cr2O3	0,02	0,02	0,03	0,01	0	0,02	0	0,02
Na2O	0	0,05	0	0,04	0	0	0,149	0,12
TOTAL	99,75	99,687	100,09	99,492	99,555	99,582	99,965	99,991
Si	7,907	7,902	7,884	7,864	7,886	7,888	7,854	7,869
Al	0,1333	0,1328	0,1486	0,1543	0,1504	0,1444	0,2341	0,1649
Ti	0,013	0,0129	0,0109	0,0163	0,017	0,0101	0,0202	0,0165
Cr	0,003	0,003	0,003	0,002	0,000	0,003	0	0,0028
Fe	4,714	4,726	4,743	4,68	4,672	4,712	1,998	1,829
Mg	3,009	2,98	2,967	3,028	3,021	2,992	2,261	2,384
Mn	0,0875	0,0936	0,1074	0,1035	0,0978	0,102	0,0341	0,0351
Ca	0,1443	0,1598	0,1639	0,1868	0,1774	0,1765	3,584	3,711
Na	0,00	0,0151	0,00	0,0114	0,00	0,00	0,0446	0,0364
%En	38	38	38	39	39	38	29	30
%Fs	60	60	60	59	59	60	46	47
%Wo	2	2	2	2	2	2	25	23

Table 4 : Chemical composition of plagioclase from the garnet-sillimanite-biotite gneisses(Pk6b, Pk8) and garnet-pyroxene gneisses (Pk2).

											Pk8									Pk2				
	47	48	50	55	57	59	64	66	71	76	121	125	126	128	129	131	132	133	158	55	56	57	58	59
SiO_2	60,74	60,76	60,90	60,35	61,94	63,87	60,44	60,57	60,22	60,45	60,09	60,88	61,12	62,32	58,96	58,26	61,17	61,79	61,36	45,79	45,54	45,67	45,40	45,87
Al_2O_3	24,92	24,96	24,76	25,37	23,62	23,78	24,82	24,42	24,66	24,84	24,84	24,46	24,43	24,04	25,70	26,56	25,06	24,77	24,90	34,11	34,04	34,99	34,93	34,86
FeO	0,06	0,13	0,04	0,01	0,00	0,00	0,01	0,00	0,02	0,01	0,01	0,01	0,00	0,00	0,00	0,01	0,00	0,01	0,00	0,115	0,186	0,168	0,333	0,482
CaO	7,29	5,45	7,08	7,81	6,41	4,57	7,38	5,74	7,85	8,67	7,61	7,36	6,55	5,15	9,61	9,71	7,42	7,32	7,35	18,3	18,3	17,96	17,88	17,79
Na_2O	6,78	5,10	6,50	6,92	7,14	8,39	6,57	5,93	6,40	5,99	6,56	6,55	6,90	7,82	5,52	5,16	5,95	6,49	6,68	1,305	1,38	1,341	1,42	1,331
K_2O	0,17	3,00	0,44	0,14	0,13	0,17	0,22	2,79	0,30	0,07	0,29	0,13	0,11	0,10	0,14	0,17	0,40	0,36	0,18	0,031	0,039	0,04	0,012	0,044
Total	99,95	99,41	99,75	100,60	99,24	100,78	99,43	99,45	99,44	100,03	99,40	99,40	99,11	99,43	99,92	99,86	100,0	100,7	100,5	99,7	99,5	100,2	100,0	100,4
Si	2,70	2,72	2,71	2,67	2,76	2,79	2,70	2,72	2,69	2,68	2,69	2,70	2,73	2,76	2,63	2,60	2,72	2,72	2,71	6,291	6,306	6,325	6,346	6,324
Al	1,30	1,32	1,30	1,32	1,24	1,22	1,31	1,29	1,30	1,30	1,30	1,31	1,29	1,26	1,35	1,40	1,29	1,27	1,30	5,646	5,618	5,622	5,591	5,599
Fe	0,002	0,005	0,00	0,00	0,00	0,01	0,00	0,00	0,01	0,01	0,01	0,00	0,00	0,00	0,01	0,01	0,01	0,00	0,00	0,014	0,022	0,02	0,039	0,057
Ca	0,35	0,26	0,34	0,37	0,31	0,21	0,35	0,28	0,38	0,41	0,35	0,35	0,31	0,24	0,46	0,46	0,35	0,33	0,35	2,754	2,745	2,701	2,678	2,674
K	0,01	0,17	0,03	0,01	0,01	0,01	0,01	0,16	0,02	0,00	0,01	0,01	0,01	0,01	0,01	0,01	0,02	0,01	0,01	0,355	0,374	0,365	0,385	0,362
Na	0,58	0,44	0,56	0,59	0,62	0,71	0,57	0,52	0,55	0,52	0,61	0,57	0,60	0,67	0,48	0,45	0,50	0,62	0,57	0,006	0,007	0,007	0,002	0,008
An %	37	30	37	38	33	23	38	29	40	44	36	38	34	27	49	50	40	34	37	88	88	88	87	88
Ab	62	51	61	61	66	76	61	54	59	55	63	61	65	73	51	49	58	65	62	11	12	12	13	12
Or	1	20	3	1	1	1	1	17	2	1	1	1	1	0	0	1	2	1	1	1	0	0	0	0

towards the SSW (Fig 2). F1 folds occur as decimetre-sized isoclinals folds with S1 as the axial plane schistosity. Their axes are roughly parallel to L1. Mineral assemblages in these metapelites are (1) Grt-Kfs-Pl-Bt-Sill-Qtz or (2) Kfs-Pl-Bt-Qtz. A D2 deformation was preferentially recorded in orthogneisses. It is characterized by steeply dipping foliation planes that are oriented roughly parallel to the general strike of the shear zone. The overall conformable nature of the foliation, either acquired during the magmatic stage or in the solid state, point to the syn-D2 emplacement of granites (actually orthogneissified). This phase is responsible for a S2 schistosity (strike N40°E) transposing S1, and favoured emplacement of granitoids along the shear zone (strike N40°E). Quartzo-felsdpathic leucosomes locally infill pressure shadows between boudins.

Strongly foliated garnet gneisses (Fig 3a) were sampled along the shear zone in Kekem area. Under the microscope, the planar and slightly anastomosing foliation planes are underlined by quartz, sheared biotite and sometimes fibrous sillimanite (Fig 3b). Quartz displays mortar textures with pervasive recrystallisation by grain boundary migration. Many quartz grains also show plastic deformation with elongation along the foliation planes. This pervasive high temperature mylonitic foliation surrounds lenticular microlithons with garnets up to 3 mm in diameter, plagioclase, K-feldspar, large and undeformed biotite and quartz. The poikiloblastic garnets enclose large biotite, plagioclase, rounded quartz, sillimanite rods and oxides and display numerous cracks. The shapes of the garnets are round to lenticular. The garnet crystals do not show an optical zoning. Some crystals of garnet show transformation to biotite and quartz at the rims (retrograde reaction).

Table 5 : Chemical composition of biotite of garnet-sillimanite-biotite gneisses (Sample Pk6b, Pk8 and by3) and Garnet-pyroxene gneisses (Sample Pk2).

Sample	Pk6b							Pk8									By3				Pk6b						Pk2				
Analyses	80	81	82	83	84	87	88	89	90	91	92	93	94	95	96	97	135	136	137	138	146	147	162	163	56	134	44	45	46	47	48
SiO_2	37,28	36,42	37,14	37,71	36,79	37,43	37,79	37,80	37,85	37,63	38,25	37,92	37,62	36,81	36,06	35,44	37,42	37,53	37,04	37,18	37,41	37,70	49,61	49,72	46,29	46,10	35,23	35,21	35,23	35,08	34,88
Al_2O_3	15,36	15,40	15,31	16,47	16,86	15,99	15,39	16,16	16,56	15,83	15,71	15,45	15,53	15,73	17,18	15,63	15,90	15,66	15,14	15,89	15,96	15,47	31,60	31,91	32,23	35,55	13,96	13,75	14,17	14,13	13,94
TiO_2	3,38	3,50	3,23	5,35	5,65	4,10	4,00	4,16	4,43	4,48	4,36	4,14	5,06	5,15	2,30	5,29	2,90	2,30	4,72	5,99	3,38	3,43	0,36	0,15	0,00	0,03	5,14	4,98	5,14	4,53	4,77
FeO	18,45	18,67	18,56	14,34	14,54	16,76	15,71	15,09	14,70	15,07	15,01	14,61	15,52	15,76	20,68	17,87	16,35	16,42	16,31	15,21	16,88	17,04	2,35	1,47	7,26	0,52	21,92	22,80	22,61	22,78	22,52
MgO	11,05	11,49	11,58	11,44	11,81	11,54	12,02	12,11	11,51	12,33	12,25	12,66	12,05	12,53	14,10	11,08	12,66	13,62	10,91	11,93	11,58	11,48	0,94	0,96	0,04	0,19	8,77	8,64	8,46	8,84	8,70
K_2O	8,83	8,75	8,56	8,91	9,13	8,78	8,61	8,75	8,71	8,78	8,66	8,73	8,52	8,57	3,65	8,72	8,73	8,18	8,79	7,17	8,70	8,80	10,53	10,35	8,26	11,69	9,59	9,60	9,70	9,63	9,58
Na_2O	0,11	0,09	0,13	0,07	0,03	0,12	0,22	0,15	0,23	0,07	0,19	0,15	0,10	0,16	0,07	0,12	0,16	0,07	0,11	0,01	0,13	0,10	0,11	0,99	0,98	0,98	0,08	0,06	0,11	0,14	0,04
Cr_2O_3	0,09	0,08	0,06	0,12	0,09	0,08	0,08	0,07	0,09	0,08	0,08	0,08	0,09	0,07	0,08	0,10	0,04	0,03	0,08	0,68	0,07	0,06	0,04	0,02	0,03	0,01	0,09	0,04	0,10	0,06	0,07
total	94,56	94,41	94,58	94,41	94,89	94,80	93,82	94,28	94,07	94,26	94,49	93,74	94,50	94,78	94,12	94,25	94,17	93,81	93,11	94,07	94,11	94,08	95,52	95,57	95,08	95,06	94,78	95,08	95,52	95,19	94,50
	bt	bt	bt	bt	bt	bt	bt	bt	bt	bt	bt	bt	bt	bt	bt	bt	bt	bt	bt	bt	bt	bt	ms	ms	ms	ms					
Mg	0,44	0,46	0,46	0,47	0,48	0,46	0,48	0,48	0,47	0,49	0,49	0,51	0,48	0,50	0,49	0,45	0,50	0,52	0,45	0,48	0,46	0,46	0,05	0,05	0,00	0,01	0,23	0,20	0,14	0,25	0,23
Fe	0,41	0,41	0,41	0,33	0,33	0,38	0,35	0,34	0,34	0,34	0,34	0,33	0,35	0,35	0,40	0,40	0,36	0,35	0,38	0,34	0,38	0,38	0,07	0,04	0,19	0,02	0,13	0,26	0,21	0,25	0,24
Ti	0,07	0,07	0,06	0,11	0,11	0,08	0,08	0,08	0,09	0,09	0,09	0,08	0,10	0,10	0,04	0,11	0,06	0,04	0,10	0,12	0,07	0,07	0,01	0,00	0,00	0,00	0,66	0,64	0,66	0,58	0,62
Al VI	0,08	0,06	0,07	0,10	0,08	0,08	0,08	0,09	0,11	0,08	0,08	0,08	0,07	0,05	0,07	0,04	0,08	0,08	0,07	0,06	0,09	0,09	0,88	0,91	0,81	0,97	0,81	0,77	0,84	0,84	0,82
K	0,98	0,98	0,98	0,99	1,00	0,98	0,96	0,97	0,96	0,99	0,97	0,97	0,98	0,97	0,97	0,98	0,97	0,99	0,98	1,00	0,98	0,98	0,98	0,87	0,85	0,89	0,09	0,09	0,10	0,10	0,10
XMg	0,52	0,52	0,53	0,59	0,59	0,55	0,58	0,59	0,58	0,59	0,59	0,61	0,58	0,59	0,55	0,53	0,58	0,60	0,54	0,58	0,55	0,55	0,42	0,54	0,01	0,39	0,42	0,40	0,40	0,41	0,41

Large undeformed biotite and feldspar occur in the pressure shadows of the porphyroblasts.

4-2. Mineral chemistry

4-2-1. Garnet and/or sillimanite-biotite gneisses

These rocks are the most abundant type in the Kekem area. They are fine- to medium- grained, grey-coloured, with alternating millimetre to centimetre scale, garnet-biotite-rich and quartzo-felsdpathic layers. They are composed of plagioclase, quartz, K- feldspar, biotite, garnet and accessories, such as apatite, zircon, monazite and oxides. The garnets in samples Pk6b, Pk8 and by3 display low contents of spessartine (at around 2 wt%) and a poor zonation of this component. Spessartine contents only slightly increase towards the garnet rims. Pyrope contents are high at around 20 wt. % with a slight decrease towards the rims. Accordingly, the garnets did not crystallize during a prograde metamorphism

Table 6: Representative major (wt%) and trace (ppm) element analyses of garnet-sillimanite-biotite gneisses (Pk6b to Pk8), garnet - pyroxene gneisses (ptnk2c to by1a) and amphibolites (Pk9 to Pk6d). By10 = Orthogneiss

Sample	By10	pk9	ke44	ke3	pk6a	pk6c	pk6d	pk6b	by3	by1b	pk8	pt nk 2c	ptnk3c	pk2	by1a
SiO_2	71,9	69,8	67,7	61,7	62,7	62,9	62,7	60,2	58,9	58,9	56,9	49,8	45,8	43,7	43,3
TiO_2	0,18	0,50	0,41	0,85	1,15	1,11	1,23	1,33	1,16	1,02	1,14	4,1	2,32	2,16	2,28
Al_2O_3	15,5	14,3	15,9	15,5	14,9	15,1	15	15,3	17,1	18,7	19,9	13,3	13,3	13,4	17,2
Fe_2O_3total	1,12	4,48	4,26	8,26	8,19	7,94	8,2	9,12	6,61	5,96	9,12	16,58	21,2	19,7	15,2
MnO	0,02	0,10	0,07	0,18	0,11	0,11	0,11	0,12	0,11	0,10	0,15	0,199	0,3	0,25	0,12
MgO	0,35	1,43	1,62	3,04	1,8	1,72	1,73	2,04	2,2	2,01	2,38	4,46	6,13	6,94	6,04
CaO	1,22	2,64	4,62	4,4	4,92	5,01	5,06	5,6	5	4,43	2,69	8,46	9,52	10,5	10,8
Na_2O	3,78	3,49	4,18	3,6	3,29	3,38	3,37	3,37	3,89	4,49	2,71	1,72	0,56	0,33	1,25
K_2O	5,06	2,33	0,67	1,27	1,65	1,62	1,57	1,7	3,42	3,41	4,38	0,61	0,5	2,36	2,59
P_2O_5	0,08	0,31	0,12	0,16	0,34	0,33	0,37	0,39	0,53	0,38	0,08	0,516	0,23	0,23	0,47
LOI	0,6	0,4	0,31	0,65	0,46	0,55	0,72	0,32	0,65	0,35	0,23	0,21	0,11	0,12	0,25
Total	99,8	99,8	99,8	99,6	99,5	99,8	100	99,5	99,6	99,8	99,7	100	100	99,7	99,5
Na_2O+K_2O	8,84	5,82	4,85	4,87	4,94	5	4,94	5,07	7,31	7,9	7,09	2,33	1,06	2,69	3,84
Al_2O_3/SiO_2	0,22	0,20	0,23	0,25	0,24	0,24	0,24	0,25	0,29	0,32	0,35	0,27	0,29	0,31	0,40
Sc		9	7	21	20	18	16	20	21	16	18	28	26	19	21
V		85	54	151	121	108	96	119	133	121	135	360	386	374	301
Cr		61	41	73	67	53	51	49	67	41	82	110	151	140	111
Co		12	13	29	27	18	15	20	23	21	24	52	55	41	48
Ni		31	27	93	61	49	47	50	87	47	90	207	225	231	201
Cu		31	35	151	54	16	38	17	15	16	12	206	191	165	189
Zn		78	51	97	91	109	101	122	135	111	147	161	155	171	131
Rb		16	6	49	42	63	61	179	187	181	195	20	25	22	18
Sr		285	356	385	331	298	251	272	351	287	354	237	231	245	218
Y		5	4	8	6	5	4	60	43	57	37	45	48	41	43
Zr		29	31	25	33	43	37	178	169	181	165	140	150	132	167
Nb		5	3	6	5	8	4	18	21	16	16	26	29	24	21
Ba		316	327	855	832	752	686	1028	1125	1051	1462	82	78	71	78
La		9,09	9,76	10,19	10,43	11,04	10,03	37,0	51,4	39,7	57,5	38,4	41,2	40,4	35,4
Ce		15,12	14,68	14,81	14,89	13,46	12,51	83,8	98,7	81,3	117	83,8	78,5	90,9	81,8
Pr		2,01	1,44	5,91	7,41	10,63	8,93	10,9	15,3	11,7	13,2	11,2	10,3	12,3	11,1
Nd		9,81	9,60	10,07	9,57	10,41	9,11	44,6	41,2	49,4	47,3	49,7	48,5	55,9	51,3
Sm		4,05	4,01	3,92	3,81	3,94	3,73	9,83	8,01	9,65	7,78	11,4	11	12,2	12,9
Eu		0,98	0,83	0,81	0,901	0,92	0,95	2,20	2,27	2,67	2,70	3,37	3,17	2,98	2,86
Gd		4,02	4,08	4,07	3,99	4,15	4,35	11,3	8,96	11,0	7,91	12,5	14,3	13,2	13
Tb		0,21	0,19	0,22	0,21	0,22	0,189	1,71	1,09	1,43	1,06	1,61	1,33	1,64	1,91
Dy		0,95	0,84	0,97	0,93	0,87	0,77	10,6	10,4	9,89	6,88	9,20	10	9,88	9,42
Ho		0,71	0,15	0,63	0,51	1,77	1,03	1,99	1,71	1,33	1,23	1,54	1,53	1,41	1,32
Er		0,97	0,75	0,93	0,92	0,97	0,81	5,57	4,01	3,94	3,44	4,25	3,97	3,98	4,21
Tm		0,1	0,11	0,10	0,14	0,19	0,11	0,81	0,73	0,65	0,51	0,57	0,55	0,62	0,51
Yb		0,67	0,69	0,63	0,71	0,72	0,733	5,47	4,02	3,87	3,06	3,20	3,19	3,33	3,18
Lu		0,31	0,38	0,37	0,33	0,27	0,31	0,74	0,58	0,51	0,49	0,48	0,42	0,41	0,45
Hf		0,87	0,77	0,92	1,03	1,32	1,36	3,86	3,79	3,73	3,81	3,42	3,01	3,21	3,54
Ta		1,43	0,70	2,73	3,45	4,64	4,05	4,87	2,35	4,46	1,40	7,47	5,68	3,47	6,42
W		0,55	0,47	0,70	0,67	0,74	0,57	0,58	0,54	0,61	0,65	0,83	0,71	0,65	0,61
Tl		0,12	0,08	0,25	0,23	0,35	0,41	0,31	0,39	0,53	0,79	0,09	0,07	0,07	0,05
Pb		6,01	6,06	5,57	5,82	5,26	5,67	5,42	21,2	4,34	33,5	2,20	2,01	2,2	1,99
Th		0,17	0,20	3,20	3,42	7,31	6,35	5,47	7,87	4,87	6,42	5,86	5,81	6,02	4,86
U		0,21	0,08	0,28	0,71	0,76	0,56	0,66	0,99	1,01	1,54	1,11	0,71	1,01	0,98
(Ce/Sm)N		0,90	0,88	0,91	0,94	0,82	0,81	2,06	2,98	2,03	2,66	1,78	1,73	1,79	1,54
(La/Yb)N		9,16	9,50	10,86	9,92	10,34	9,24	5,59	8,63	6,93	9,80	8,11	8,72	8,18	7,52
(Gd/Yb)N		4,85	4,76	5,20	4,54	4,65	4,80	2,05	1,80	2,29	2,02	3,15	3,63	3,21	3,30
(Gd*Sm)N		517	520	508	483	520	516	3536	2281	3362	2765	4500	4995	5139	5306
Eu/Eu*		0,74	0,63	0,62	0,71	0,69	0,72	0,64	0,82	0,79	0,88	0,87	0,77	0,72	0,68

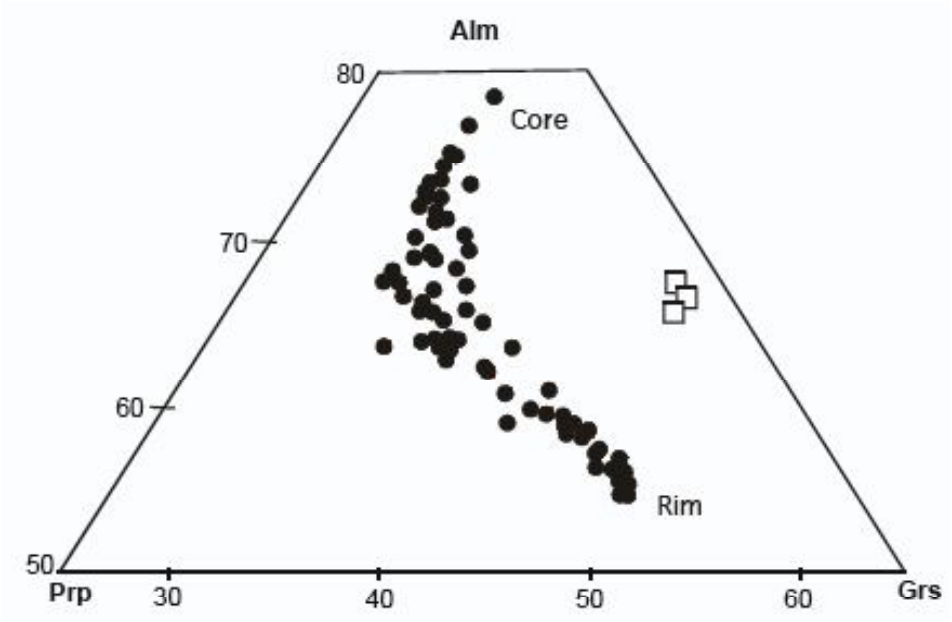

Fig. 4: Almandine (Alm)- pyrope (Prp) -grossular (Grs) diagram showing composition of the garnet and zoning garnet. Garnet-sillimanite-biotite gneisses (●); garnet-pyroxene gneisses (❒).

wherein typical increase in Mg and decrease Mn (Spear, 1993) are expected. It is more likely that the garnets crystallized at the maximal temperature and possibly underwent high-temperature homogenisation. Zonation of the grossular component is also poorly developed and range at around 5 - 8 wt% and it is almost constant within single porphyroblasts. This Ca zonation is inversely matched by the zonation in Fe (Fig 4). This gives evidence that at least the Fe, Mg and Ca components in the garnet were not homogenised at high temperatures but should reflect a growth zonation trend.

Biotite elongated in the foliation in sample Pk6b, Pk8 has X_Mg of 0.52 - 0.55 and Ti between 0.2 -0.3. In sample by3, the X_Mg of biotite is variable and dependent on the microstructural position of the crystals. Biotite in garnet pressure shadows has X_{Mg} around 0.46 and Ti of 0.25; biotite along the foliation has XMg of 0.52 and Ti of 0.20, while isolated biotite flakes enclosed in plagioclase have X_{Mg} values of 0.57 with low Ti of 0.12. It is suggested that the isolated biotite represents a generation which crystallized at low temperatures during an early stage of the metamorphic evolution whereas the other biotite crystallized at high temperatures and coexisted with the garnets.

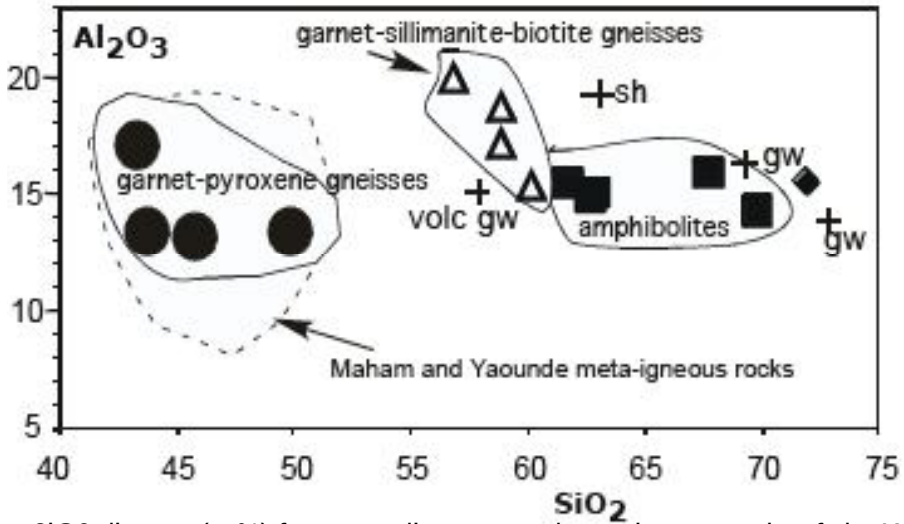

Fig. 5: Al2O3 versus SiO2 diagram (wt%) for metasedimentary and meta-igneous rocks of the Kekem area. : garnet-sillimanite-biotite gneisses; ● : garnet-pyroxene gneisses; ■ : amphibolites; sh: average shales; gw: greywackes; volc. gw: volcanogenic greywackes; from Taylor and McLennan (1985).

The composition of plagioclase enclosed in garnet in sample Pk6b, Pk8 is An30-40. In large matrix plagioclase porphyroblasts a zonation from An25 in the core to An44 in the rim can be observed. Similar compositional variations and zonation of plagioclase were found in sample by3.

4-2-2. Meta-igneous rocks

They are fine to medium-grained, dark coloured rocks, granoblastic rocks displaying a weak layering (Fig 3d). They are composed of plagioclase, orthopyroxene, clinopyroxene, garnet, biotite, K-feldspar, and quartz. Accessories are apatite, ilmenite and zircon. Garnet are unzoned and have a constant composition. All garnets are on the whole almandine (65 - 66%), grossular (20-21%), pyrope (12 - 13%), solid solution and low spessartine ($\leq$2%) components (Table 2). Plagioclase has a constant An content (An87-88; table 4). Clinopyroxene is generally subcalcic ferro-augite in composition (X_{Ca} = 0.23-0.25; X_{Mg} = 0.29-0.30; X_{Fe} = 0.46-0.47; Table 3). Orthopyroxene is orthoferrosilite in composition (X_{Fe} = 0.59-0.60; X_{Mg} = 0.39-0.38; X_{Ca} = 0.2; Table 3). Biotite has X_{Mg} of 0.40-0.42. Some of them contain abundant retromorphic poikiloblastic hornblende replacing pyroxenes. The other types are much more restricted and occur as discontinuous, often boudinaged, layers in the metasediments. They comprises (table 1): (i) amphibolites made up of plagioclase, quartz, K-feldspar, pyroxene, biotite and amphibole; (ii) pyroxenites composed either of orthopyroxene, garnet and quartz. Accessories are, in all rock types, apatite, zircon and oxides.

4-3. Whole-rocks geochemistry

4-3-1. Metasedimentary rocks

Representative major and trace element compositions of metasediments are given in Table 6. These rock types define a chemical trend parallel to that of average shales (Fig 5), but with a slightly lower Al_2O_3/SiO_2 ratio. Sillimanite-garnet-biotite gneisses display Fe_2O_3, MgO and TiO_2 contents correlated to Al2O3 and inversely correlated to SiO_2 suggesting that they were initially

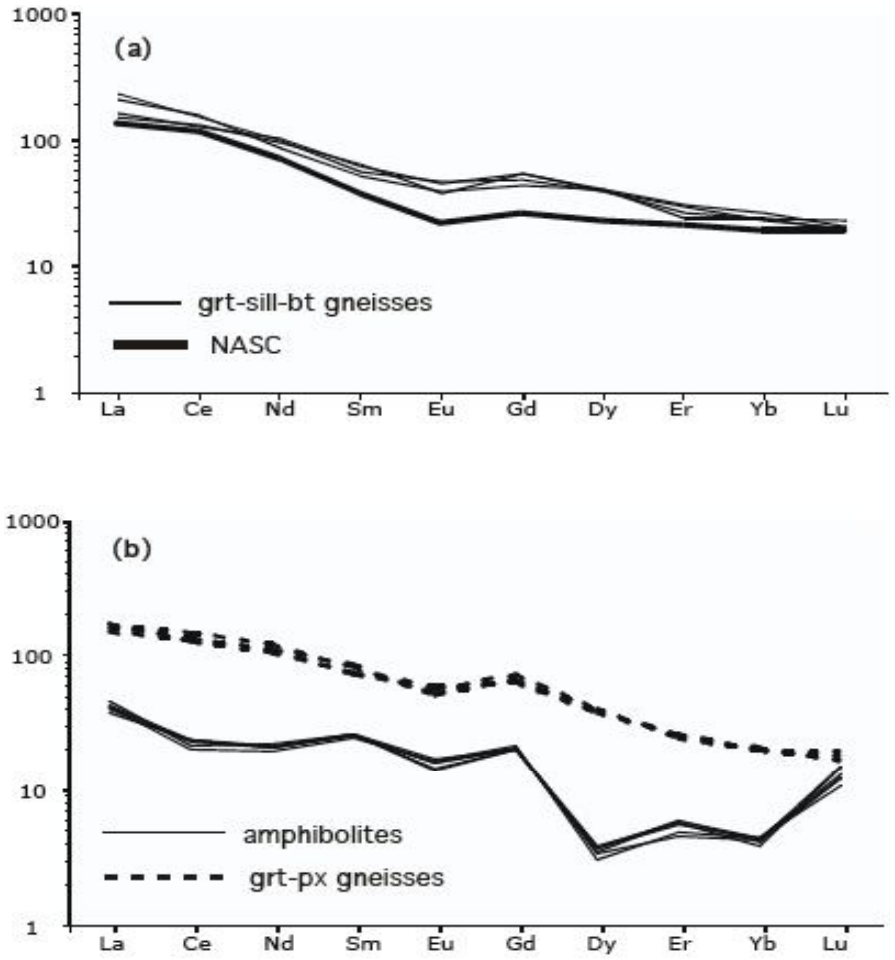

Fig. 6: Chondrite-normalised REE patterns for metasedimentary (a) and meta-igneous (b) rocks of the Kekem area. North American shale composite (NASC) from Haskin et al., 1968. The normalising values are from Evensen *et al*., 1978.

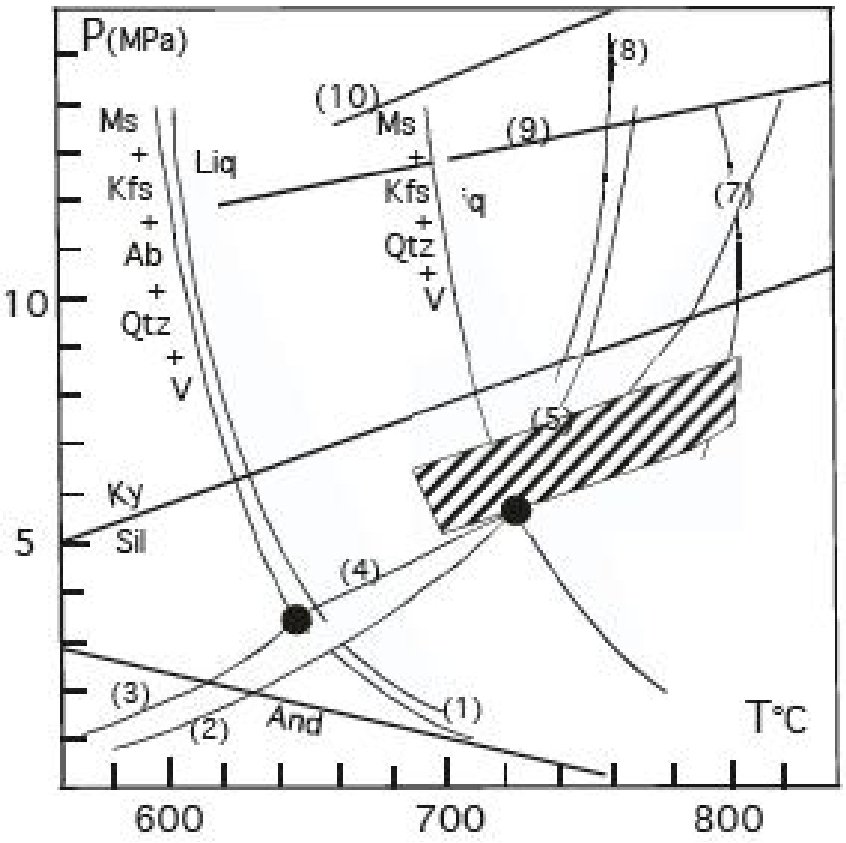

Fig. 7: Synthetic P-T-paths diagram from the Kekem gneisses. Stability field of Aluminosilicates from Holdaway (1971). Stability curves from Thompson and Algor (1977) : (2) Ms + Qtz = Kfs + Als + V ; (4) Ms + Qtz + Liq = Kfs + Sil + V ; (5) Ms + Qtz + V = Als + Liq; (6) : Ms + Qtz = Ky + Liq. From Vielzeuf and Holloway (1988) : (7) Bt + Als + Qtz + V = Liq + Grt; (8) Ms + Bt + Qtz + V = Ky + Liq; (9) Pl + Hbl = Omp + Grt; (10) PlAn30 + V = Ky + Zo + Qtz.

composed of a quartz-clay mixture. Their TiO_2 contents (1.02-1.33%) are similar to those of post-Archean shales (0.7-1.03%: Taylor and McLennan, 1985) and Cameroon Neoproterozoic shales (0.98 - 1.29%: Nzenti et al., 1988; Ngnotué et al., 2000), but their CaO (2.69 - 5.6%) and Na_2O (2.71 - 4.49%) contents are higher than average terrigeneous shales (CaO = 1.3%, Na_2O = 1.2%: Taylor and McLennan, 1985). Their rare earth element (REE) patterns[151<LaN<235, 23<YbN<27, Fig 6a] are closely similar to the North American shales composite (NASC: Haskin et al., 1998). These gneisses, displaying major and trace element contents similar to those of the Neoproterozoic garnet gneisses in Cameroon (Nzenti et al., 1988; Ngnotué et al., 2000), can be regarded as metasediments with significant proportion of clay.

4-3-2. Meta-igneous rocks

Garnet-pyroxene gneisses are mainly mafic in composition (Table 6), with a silica contents ranging from 43.3 to 49.8% and a rather constant Al content (13.3%). The higher Fe_2O_3 (15.2 to 21.2%) and MgO (4 to 7%) contents together with high Cr (110 to 151ppm) and Ni (201 to 231ppm) contents and constant Y and Nb contents suggest that their more mafic composition is related to accumulation of pyroxene rather than a less differentiated nature. Their REE patterns (Fig 6b) are slightly fractionated (La_N/Yb_N = 7.52 - 8.72), LREE enriched (Ce_N/Sm_N= 1.53-1.79), and display a negative Eu anomaly (Eu/Eu* = 0.68 - 0.87). Pyribolites are characterized by high Al_2O_3, Na_2O, K_2O, Ba and Sr but low MgO, CaO, Nb and Y contents (table 6). The REE patterns (Fig 6) are less fractionated (La_N/Yb_N = 9.16-10.86; Gd_N/YbN = 4.54-5.20) than those of the garnet -pyroxene gneisses. Negative Eu anomalies (Eu/Eu* = 0.62-0.74). Major and trace element data are limited and do not allow a detailed discussion of their protoliths.

4-4. Geothermobarometry

4-4 -1 Mineral assemblages

Deformation-recrystallisation relationships allow three successive mineral paragenesis stages to be distinguished

in the Kekem area. An early stage consists of Bt + Sill +Qtz + Gr (metasediments) and Qtz + Pl + Bt (metabasites) assemblages occurring in garnet porphyroblasts as inclusions. The main stage is associated with the D1 structures and displays the following phase assemblages:

(1) Qtz + Pl + Kfs + Grt + Sill ± Bt + Gr, Qtz + Grt + Kfs + Pl ± Bt + Gr and Qtz + Ms + Kfs + Grt ± Sill in metapelitic gneisses;

(2) Grt + Opx + Cpx + Pl + Qtz, Grt + Opx + Cpx + Pl + Qtz ± Hbl in garnet-pyroxene gneisses and Grt + Cpx + Qtz + Pl + Hbl + Bt in amphibolites.

Late phase assemblages are characterised by the widespread development of biotite and muscovite in the metapelites and of amphibole and biotite in the meta-igneous rocks. These data allow several points to be emphasized:

(i) The presence of early assemblages containing sillimanite as the only Al-silicate and the development of the sillimanite in the late stages are consistent with a clockwise P-T-time path.

(ii) The persistence of Qtz + Pl + Grt + Sill and Ms + Qtz Sill assemblages in association with leucosomes in metapelites gneisses indicate that temperature conditions did not exceed 800°C, whereas the presence of sillimanite crystals in leucosomes suggest that temperatures were higher than 750°C (Fig 7).

The data imply a high-temperature amphibolite-facies metamorphism along a clockwise P-T path. The recorded P-T involves a marked variation in pressure, which is typical of collisional crustal thickening.

(iii) The overall stability of sillimanite at temperatures higher than 750°C is consistent with the stability of the Grt + Cpx assemblages in metabasites .

4-4 -2 Thermobarometry

As single garnet traverses may not have passed through the entire garnet core region and the porphyroblasts may display zonation gaps or may show only a part of the complete garnet chemical evolution, in the case of the Kekem metapelites only one garnet porphyroblasts in sample Pk8b displays a marked zonation, namely in Ca. An application of garnet-biotite Fe-Mg exchange geothermometer and garnet-plagioclase Ca-net-transfer geobarometers in progressively deformed metapelites with markedly zoned garnet requires analyses from mica and plagioclases corresponding to early (i.e. core) and successively later (i.e. towards rim) stages of the garnet growth. When compositional zoning of garnet in metapelites is a product of continuous reactions involving garnet, mica, plagioclase, aluminosilicates and quartz of low-variation assemblages (Tracy, 1982), it reflects finite temporal and spatial domains of equilibration. Moreover, when coexistent minerals (mica and plagioclase) are preserved within a microstructural domain or occur as inclusions which can be correlated with matrix phases (St-Onge, 1987), their chemical compositions in such localised equilibrium allow to evaluate successive P and T or P-T changes for consecutive stages of garnet growth by geothermobarometry (Triboulet and Audren, 1985; Schulz, 1990; 1993). The core of zoned garnet and its inclusions should represent an early stage of the metamorphic evolution. Accordingly, P and T for crystallization of Mg-rich garnet rims have been calculated by the garnet-biotite thermometer of Battacharya *et al*. (1992) in combination with the GASP (garnet-aluminosilicates-plagioclase-quartz barometer, Holland & Powell, 1990; Holdaway, 2001), involving an internally consistent thermodynamic data set, the updated activity models for garnet (Ganguly *et al*., 1996), for plagioclase (Powell & Holland, 1993), and involving sillimanite.

Temperature and pressure estimates of the rocks were obtained using these three procedures :

1- Geothermobarometry based on cation-exchange and net transfer reactions in preserved garnet-bearing assemblages has been used to reconstruct a decompression path at high temperatures preceding the mylonitization.

2- Grt-Cpx/Opx-Pl-Qtz barometer of Newton and Perkin´s (1982) as modified by Raith *et al.* (1983), and temperatures from the Grt-Cpx of Berman et al (1995), Grt-Al-Opx thermometers of Aranovick and Bermann (1997) These thermometers use the Fe and Mg exchange equilibrium between garnet and pyroxene and Al_2O_3 content of Opx equilibrium with garnet. Temperatures and pressures estimates range between 700° and 800°C and 5 to 8Kb (Fig 7), respectively.

3 - Grt-Pl-Sill-Qtz barometer of Newton and Haselton (1981) with the garnet solid solution model of Ganguly and Saxena (1984), Grt-Bt thermometer of Ferry and Spear (1978). This thermometer uses the Fe and Mg exchange equilibrium between garnet and biotite. Biotite and garnet from paragneisses have, respectively, low Ti and Ca and Mn contents allowing us to use the Grt-Bt thermometer. Barometric estimates

are consistent with the petrogenetic grid and indicate that the P-T conditions of the highest grade stage were 800°C and 7Kbar.

5. DISCUSSION AND CONCLUSION

The main lithology in the Kekem area corresponds to a shale-dominated metasedimentary sequence intruded by the magmatic complex comprising more or less orthogneissified granitoids. Meta-igneous rocks comprise garnet-pyroxene gneisses and amphibolites with chemical patterns similar to those of the other Pan-African regions such as the Maham III and Banyo mafic meta-igneous rocks. This therefore, suggests that the geodynamic context envisaged for the Maham III and Banyo Formation (Tanko Njiosseu *et al*., 2005; Nzenti, 1998b, Nzenti *et al*., 2007) can be extended farther west towards central Cameroon domain of the fold belt.

The behaviour of elements and thermobarometric estimates in the Kekem area show that zoned garnets have undergone an evolution and growth during prograde metamorphism and then resorption during retrograde metamorphism. This behaviour is identical to that of many garnets described in literature (Bethune *et al*., 1968; Blackburn et Navarro, 1977; Thompson *et al*., 1977; Karabinos, 1984; Nzenti, 1992; Massoudi *et al*., 2006). This evolution is compatible with two growth phases: a growth phase at increasing temperature and decreasing pressure and another phase at decreasing temperature and pressure.

The Pan-African tectonic evolution of the Kekem area appears to result from a major tectono-metamorphic event. The early stage (D1) characterized by flat-lying schistosity, isoclinals folds and nearly horizontal stretching lineation, corresponds to tangential movements. Phase assemblages indicate that the conditions of metamorphism culminated during this stage at temperature around 760-800°C and pressures around 8Kb. The subsequent evolution (D2), marked by decompressional event is accompanied by partial melting and, then, retrogression of metamorphic assemblages (700°C/5kbar). The D2 phase is also accompanied by the emplacement of the syntectonic granitoids, similar to those described in the central domain in the Cameroon Pan-African Fold Belt (Djouka-Fonkwé *et al*., 2008; Njiekak *et al*., 2008; Nzenti *et al*., 2006; Tanko Njiosseu et al., 2005; Tagne-Kamga, 2003; Nguiessi *et al*., 1997). This tectonic evolution and the conditions of recrystallisation are close to those reported for the Maham III and Banyo gneisses in Cameroon Central domain (650-750°C, 5-7Kb: Nzenti, 1998; Tanko Njiosseu *et al.,* 2005; Ngnotué *et al*., 2000).

The Pan-African peak pressures in the study area and another part of the fold belt (Maham III, Banyo etc.) are very homogeneous and thus imply that the whole central part of the Neoproterozoic belt which is presently exposed represents the same crustal level.

It is interesting to compare the results of the Kekem area (southwestern part of the central domain and inside the Cameroon Central Shear Zone) with data from the Banyo area (Ngako *et al*., 1991; Nzenti, 1998b; Nzenti *et al*., 2007) located to the north of the Cameroon Central Shear Zone (CCSZ, Fig 1), Tonga area (Tanko Njiosseu *et al*., 2005) located immediately to the East of the study area and at south of CCSZ and Kombé-II area near Bafia town (Ganwa *et al*., 2008) to the south of the study area. These areas consists of an assembly of fragments of a Paleoproterozoic continental crust recrystallised under high-grade granulites and amphibolites-facies conditions at ca 2100Ma, and of metasediments displaying phase assemblages recrystallised under low pressure conditions (650-750°C, 0.5-0.7GPa) during the Neoproterozoic Orogeny. This allows one to emphasise the contrasted Pan-African metamorphic evolution between the metasediments of the Kekem area (high pressure and lower pressure conditions) and those located to the east and south (low pressure conditions).

This leads us to constrain several points that should be carefully considered in any large-scale geodynamic reconstruction of the Neoproterozoic Orogeny to the north of the Congo Craton:

(i) Paleoproterozoic continental crust was involved in the PANEFB from the south (Nyong) to the north (Poli area). This implies that the Pan-African sedimentary series were deposited on an old Paleoproterozoic continental crust extending up to north Cameroon.

(ii) The contrasted metamorphic evolution between the different series to the west, south and those of the north of the CCSZ, and the clockwise P-T-t path implies an important thickening of the crust during tangential tectonics. Therefore, the CCSZ is not simply that of late Pan-African transcurrent (Ngako *et al*., 1991) or transpressive shear zone as commonly considered (Nzenti *et al*., 1994; 1999; Ngako *et al*., 2003; Kankeu et al., 2006), but appears to have been formerly a major thrust zone (Ngnotué et al., 2000; Tanko Njiosseu *et al*., 2005; Nzenti *et al*., 2007).

ACKNOWLEDGEMENTS

Mineral-chemical analyses were possible by electron microprobes hosted at Chair of Mineralogy, University of Erlangen-Nuernberg and at University of Mining and Technology in Freiberg/Saxony and at Göttingen Zentrum Geowissenschaften, Abt. Geochemie, University of Göttingen. Financial support from the Deutch Ministry of Cooperation is acknowledged.

VI. REFERENCES

Aranovich, L.Y. & Berman, R.G., 1997. A new garnet-orthopyroxene thermometer based on reversed Al2O3 solubility in FeO-Al2O3-SiO2 orthopyroxene. Amer. Miner., 82, 345-353.

Berman, R.G., Aranovich, L.Y., Pattison, D.R.M., 1995. Reassessment of the garnet-clinopyroxene Fe-Mg exchange thermometer: II. Thermodynamic analysis. Contrib. Mineral. Petrol., 119, 30-42.

Bethune, P. DE, Laduron, D., Martin, H., Theunissen, K., 1968. Grenats zonés de la zone du Monte Rose (Valle Anzasca, Prov. de Novara, Italie). Bull. Suisse de Minéralogie et Pétrographie, 48, 437 - 454.

Bhattacharya, A., Mohanty, L., Maji, A., Sen, S.K. & Raith, M., 1992. Non-ideal mixing in the phlogopite-annite binary: constraints from experimental data on Fe-Mg partitioning and a reformulation of the garnet-biotite geothermometer. Contrib. Mineral. Petrol., 111, 87-93.

Blackburn, W.H. & Navarro, 1977. Garnet zoning and polymetamorphism in the eclogitic rocks of Isla de Margarita, Venezuela. Can. Mineralogist, 15, 257 - 266.

Caby, R., Sial, A.N., Arthaud, M., Vauchez, A., 1991. Crustal evolution and the Brasiliano orogeny in northeast Brazil, in: Dallmeyer and Lécorché (Ed), The west African orogens and circum-Atlantic correlatives, Springer-Verlag , pp. 373-397.

Castaing, C., Feybesse, J.L., Thieblemont, D., Triboulet, C.& Chevremont, P., 1994. Paleogeographical reconstructions of the Pan-African/Brasiliano orogen: closure of an oceanic domain or intracontinental convergence between major blocks. Precambr. Res., 69, 327-344.

Djouka-Fonkwe, M. L., Schulz, B., Tchouankoué J.-P, Nzolang, C., 2008. Geochemistry of the Bafoussam Pan-African I- and S-type granitoids in western Cameroon. Journ. Afr. Earth Sci., 50, 148-167.

Evensen, N.M., Hamilton, P.J., O´Nions, R.K., 1978. Rare-earth abundances in chondritic meteorites. Geochi. Cosmochi. Acta, 42, 1199-1212.

Ferry, J.M. & Spears, F.S., 1978. Experimental calibration of the partitioning of Fe and Mg between biotite and garnet. Contrib. Mineral. Petrol., 66, 113 - 117.

Ganguly, J. & Saxena, S.K., 1984. Mixing properties of aluminosilicates garnets: constraints from natural and experimental data, and applications to geothermo-barometry. Am. Miner. 69, 88 - 97.

Ganguly, J., Cheng, W. & Tirone, M., 1996. Thermodynamics of aluminosilicates garnet solid solution: new experimental data, an optimized model, and thermometric applications. Contrib. Mineral. Petrol, 123,37-151.

Ganwa, A., Frisch, W., Siebel, W., Cosmas, S.K., Mvondo, O.J., Satir, M., Tchakounte, N.J., 2008. Zircon 207Pb-206Pb evaporation ages of Pan-African metasedimentary rocks in the Kombé-II area (Bafia Group, Cameroon): constraints on protolith age and provenance. Journ. Afr. Earth Sci., 51, 77-88.

Hartmann, G., 1994. Late-medieval glass manufacture in the Eischsfeld region. Chemie der Erde,54, 103-128.

HaskinN, L.A., Haskin, M.A., Frey, P.A., Wildman, T.R., 1968. Relative and absolute terrestrial abundance of the rare-earth. In: Ahrens, L.H. (ed.), Origin and the distribution of elements. Pergamon Press, Oxford, pp889-912.

Henoc, J. & Tong, M., 1978. Automatisation de la microsonde. J. Microsc. Spectrosc. Electron., 3, 247-254.

Holdaway, M.J., 1971. Stability of andalusite and the aluminium silicate phase diagram. Am. Journ. Sci., 271, 97 - 131.

Holdaway, M. J., 2001. Recalibration of the GASP geobarometer in light of recent garnet and plagioclase activity models and versions of the garnet-biotite geothermometer. Amer. Mineral., 86, 1117-1129.

Holland, T. J. B. & Powell, R., 1990. An enlarged and updated internally consistent thermodynamic dataset with uncertainties and correlations: the system K2O-Na2O-CaO-MgO-MnO-FeO-Fe2O3-Al2O3-TiO2-SiO2-C-H2-O2. Jour. Metamorphic Geol., 8, 89-124.

Karabinos, P., 1984. Polymetamorphic garnet zoning from southeastern Vermont. Am. Jour. Sci., 284, 1008 - 1025.

Kretz, R., 1983. Symbols for rock-forming minerals. Am. Miner., 68, 277-279.

Massoudi, F., Mehrabi, B. & Mahmoudi, SH., 2006. Garnet (Alandine-Spessartine) growth zoning and its application to constrain metamorphic history in Dehsalm complex, Iran. Jour. Sci., Islamic Republic of Iran, 17, 235-244.

Nedelec, A., Macaudiere, J., Nzenti, J.P., Barbey, P., 1986. Evolution structurale et métamorphique des schistes de Mbalmayo (Cameroun). Implications pour la structure de la zone mobile panafricaine au contact du craton du Congo. C. R. Acad. Sci. Paris, Ser II, 303, 75-80.

Newton, R.C., Haselton, H.T., 1981. Thermodynamics of the garnet - plagioclase - Al2SiO5 - quartz geobarometer. In: Newton C., Navrotsky A and Wood B.J. (eds), thermodynamics of minerals and melts, Springer, New York , pp. 129 - 145.

Newton, R.C. & Perkins, D., 1982. Thermodynamic calibration of geobarometers based on the assemblages garnet - plagioclase - orthopyroxene (clinopyroxene) - quartz. Am. Miner., 67, 203 - 222.

Ngako, V., Jegouzo, P., Nzenti J.P., 1991. Le Cisaillement Centre Camerounais. Rôle structural et géodynamique dans l'orogenèse panafricaine. C. R. Acad. Sci., 313, 457-463.

Ngako, V., Affaton, P., Nnange, J.M., Njanko, T., 2003. Pan-African tectonic evolution in central and southern Cameroon : transpression and transtension during sinistral shear movements. Jour. Afri. Earth Sci., 36, 207-214.

Ngnotue, T., Nzenti, J.P., Barbey P. ET Tchoua, F. M., 2000. The Ntui Betamba high grade gneisses : a Northward extention of the pan-African Yaoundé gneisses in Cameroon. Jour . Afri. Earth Sci., 31, 369-381.

Nguiessi, T.C., Nzenti, J.P., Nsifa, E.N., Tempier, P., Tchoua, F.M., 1997. Les granitoïdes calco-alcalins, syncisaillement de Bandja dans la chaîne panafricaine Nord-Equatoriale au Cameroun. C. R. Acad. Sci., 325, 95-101.

Njiekak, G., Dorr, W., TchouankoueE, J. P., Zulauf, G., 2008. U-Pb zircon and microfabric data of (meta) granitoids of western Cameroon: constraints on the timing of pluton emplacement and deformation in the Pan-African belt of Central Africa. Lithos, 102, 460-477.

Nzenti, J.P., 1992. Prograde and retrograde garnet zoning at high pressure and temperature in metapelitic and grenatite rocks from Yaoundé. Journ. Afr. Earth Sci., 15. 73 - 79.

Nzenti, J.P., 1998a. Neoproterozoic alkaline meta-igneous rocks from the Pan-african North Equatorial fold belt (Yaoundé, Cameroon) : biotitites and magnetite rich pyroxenites. Jour. Afri. Earth Sci., 26, 37-47.

Nzenti, J.P., 1998b. L'Adamaoua panafricain (région de Banyo) : une zone clé pour un modèle de la chaîne panafricaine nord-équatoriale au Cameroun. Thèse Doctorat d'Etat, Université Cheikh Anta Diop -Université Nancy I , Sénégal-France.

Nzenti, J.P.; Barbey, P., Jegouzo, P. & Moreau, C., 1984. Un nouveau exemple de ceinture granulitique dans une chaîne protérozoique de collision : les migmatites de Yaoundé au Cameroun. C. R. Acad. Sci., Paris, 299, 1197-1199.

Nzenti, J.P., Barbey, P., Macaudière, J. & Soba, D., 1988. Origin and evolution of the late precambrian high-grade Yaoundé gneisses (Cameroon). Precambr. Res., 38, 91-109.

Nzenti, J.P., Barbey, P., Bertrand, J. & Macaudière, J., 1994. La chaîne panafricaine au Cameroun : cherchons suture et modèle. 15ème RST, Nancy, Société Géologique France, édit. Paris, abstract, p.99.

Nzenti, J.P., Njanko, T., Njiosseu, E.L.T. & Tchoua, F.M., 1998. Les domaines granulitiques de la chaîne panafricaine Nord-Equatoriale au Cameroun. In géologie et environnement au Cameroun, Vicat et Bilong eds. collect., GEOCAM 1 : 255-264.

Nzenti, J. P., Barbey, P., Tchoua, F.M., 1999. Evolution crustale au Cameroun : éléments pour un modèle géodynamique de l'orogenèse néoprotérozoïque. In : Vicat J.P. et Bilong (eds), Géologie et environnements au Cameroun, collect. GEOCAM 2, pp.397-407.

Nzenti, J.P., Kapajika, B., Worner, G. & Lubala, T.R., 2006. Synkinematic emplacement of granitoids in a Pan-African shear zone in Central Cameroon. Jour. Afri. Earth Sci., 45, 74-86.

Nzenti, J. P., Njiosseu Tanko, T. E. L., Nzina-Nchare A., 2007. The metamorphic evolution of the Paleoproterozoic high-grade Banyo gneisses (Adamawa, Cameroon, Central Africa). J. Cam. Acad. Sci., 7, 95-109.

Nzolang, C., Kagami, H., Nzenti J.P., & Holtz, F., 2003. Geochemistry and preliminary Sr-Nd isotopic data on the Neoproterozoïc granitoids from the Bantoun area, west Cameroon: evidence for a derivation from a paleoproterozoïc to Archean crust. Polar Geosci., 16, 196-226.

Penaye, J., Toteu, S.F., Van Schmus, W.R. & Nzenti, J.P., 1993. U-Pb and Sm-Nd preliminary geochronologic data on the Yaoundé series, Cameroon : re-interpretation of the granulitic rocks as the suture of a collision in the "centrafrican" belt. C. R. Acad. Sci. Paris, 317, 789-794.

Powell, R. & Holland T. J. B., 1993. On the formulation of simple mixing models for complex phases. Amer. Mineral., 78, 1174-1180.

Raith, M., Raase, P., Ackermand, D. & Lal, K.R., 1983. Regional geothermometry in the facies terrane of south India. Trans. Roy. Soc. Edingburgh Earth Sci., 73, 221 - 244.

Schulz, B., 1990. Prograde-retrograde P-T-t-deformation path of Austroalpine micaschists during Variscan continental collision (Eastern Alps). Jour. Metam. Geol., 8, 629-643.

Schulz, B., 1993. P-T-deformation paths of Variscan metamorphism in the Austro-alpine basement: controls on geothermobarometry from microstructures in progressively deformed metapelites. Swiss Bull. Mineral. Petrol., 73, 257-274.

Soba, D., 1989. La série de Lom: étude géologique et géochronologique d´un bassin volcano-sédimentaire de la chaîne panafricaine de l´Est du Cameroun. Thèse de Doctorat d´Etat, Université de Paris VI, France, 198pp.

Spear, F. S., 1993. Metamorphic phase equilibria and Pressure-Temperature-Time Paths. Mineralogical Society of America Monograph Series, 1, 799pp, Washington DC.

St-Onge, M. R., 1987. Zoned poikiloblastic garnets: P-T paths and synmetamorphic uplift through 30 km of structural depth, Wopmay orogen, Can. Jour. Petrol., 28, 1-21.

Tagne Kamga, G., Mercier, E., Rossy, E., Nsifa, N.E., 1999. Synkinematic emplacement of the Pan-African Ngondo igneous complex (west Cameroon, Central Africa). Jour. Afr. Earth Sci., 28, 675-691.

Tagne-Kamga, G., 2003. Petrogenesis of the Neoproterozoic Ngondo plutonic complex (Cameroon, west central Africa): a case of late-collisional ferro-potassic magmatism. Jour. Afr. Earth Sci., 36, 149-171.

Tanko Njiosseu, E.L., Nzenti, J.P., Njanko, T., Kapajika, B. & Nedelec, A., 2005. New U-Pb zircon ages from Tonga (Cameroon): coexisting Eburnean-Transamazonian (2.1 Ga) and Pan-African (0.6 Ga) imprints. C. R. Géosci., 337, 551-562.

Taylor, S.R. & MCLeannan, S.M., 1985. Greywackes : provenance and tectonic significance. In : Taylor, S.M., McLennan, S :M : (eds.), The continental crust : its composition and evolution. Blackwell, Oxford, pp. 117-142.

Tchapchet Tchato, D., 2000. Contribution à l'étude géologique de la région de Kékem (Ouest-Cameroun). Mémoire de Maîtrise, Université de Yaoundé I, 51p.

Tchapchet Tchato, D., 2001. Les marqueurs de cisaillement dans les orogènes: L'exemple des métamorphites de la région de Kékem (Ouest- Cameroun). Mémoire de D.E.A, Université de Yaoundé I, 46p.

Tchaptchet Tchato D., Schulz B., Nzenti, J. P., 2008. Electron microprobe (EMP) monazite dating and P - T data of the Neoproterozoic metamorphic and mylonitic events in the Kekem area, Cameroon North Equatorial Fold belt. Neues Jahb. Palaontol. (submitted).

Thompson, A.B., Algor, J.R., 1977. Model systems for anatexis of pelitic rocks : I. Theory of melting reactions in the system $KAlO_2$-$NaAlO_2$-$Al2O_3$-SiO_2-H_2O. Contrib. Mineral. Petrol., 63, 247-269.

Thompson, A.B., Tracy, R.J., Lyttle, P.T., Thompson, J.B.JR., 1977. Prograde reaction histories deducted from compositional zonation and mineral inclusions in garnet from the Gassets shist, Vermont, U.S.A. Am. Jour. Sci., 277, 1152 - 1167.

Toteu, S.F., Michard A., Bertrand, J.M. & Rocci, G., 1987. U/Pb dating of Precambrian rocks from northern Cameroon, orogenic evolution and chronology of the Panafrican belt in Central Africa. Precambrian Res., 37, 71 - 87.

Toteu, S.F., Van Schnus, W.R., Penaye, J. Michard A., 2001. New U-Pb and Sm-Nd data from north-central Cameroon and its bearing on the pre-Pan African history of central Africa. Precambrian Res., 108, 45-73.

Toteu, S.F., Penaye, J., Poudjom -Djomani, Y., 2004. Geodynamic evolution of the pan-african Belt in central Africa with special to Cameroon. Can. J. Earth Sci.,41, 73-85.

Tracy, R. J., 1982. Compositional zoning and inclusions in metamorphic minerals. In: Mineralogical Society of America Reviews in Mineralogy volume 10. Characterization of metamorphism through mineral equilibria (ed Ferry, J. M.), pp. 355-397. Mineralogical Society of America,Washington DC.

Triboulet ,C. & Audren, C., 1985. Continuous reactions between biotite, garnet, staurolite, kyanite-sillimanite-andalusite and P-T-time-deformation path in micaschists from the estuary of the river Vilaine, South Brittany, France. Jour. Metam. Geol., 3, 91-105.

Received:05/01/2009

Accepted: 11/06/2009